Supplementary figure legends

Figure 1. Salt concentration-dependent self-oligomerization of Par-3 NTD. (A&B) $^{1}H,^{15}N$ HSQC spectra of the wild-type Par-3 NTD recorded with low (panel A, 100 mM NaCl) and high (panel B, 2 M KCl) salt concentrations in the sample buffer. (C) $^{1}H,^{15}N$ HSQC spectrum of V13D NTD recorded in the presence of 100 mM NaCl.

Figure 2: Substitution of Val13 with Asp has minor effect on the overall structure of Par-3 NTD. (A) Overlay plot of the HSQC spectra of the wild type NTD and V13D NTD. High concentration of salt (2 M KCl) and low concentration of protein (<0.1 mM) was necessary to keep the wild type NTD as a monomer. Except for the residues surrounding Val13, the rest of the peaks from the two spectra overlap well with each other. (B) Mapping the chemical shift differences of the wild type NTD and V13D NTD on to the 3D structure of the NTD monomer. The colored residues experience observable shift differences upon mutation of Val13. The side chain of Val13 is drawn in explicit atomic representation.

Figure 3. Electrostatic potential surface properties of the V13D and D70K point mutations of NTD. (A)&(B) Substitution of Val13 with a negatively charged Asp significantly reduced positive charge potential in the "B1" region of Par-3 NTD. In this diagram, the positive charge potential is in blue; and the negative charge potential is in red. (C)&(D) Substitution of Asp70 with a Lys disrupted the negatively charged surface in the "A1" region in the Par-3 NTD.

Figure 4. Interaction of V13D NTD with D70K NTD measured by fluorescence spectroscopy. In this assay, the IAEDANS-labeled D70K NTD (1 μM) was titrated with increasing concentration of unlabeled V13D NTD, and the polarization value of the IAEDANS-labeled D70K NTD was measured at each titration point. The data demonstrate that the interaction between the two monomeric versions of NTD can be specifically disrupted by high concentrations of salt.

Figure 5. Mapping of the interaction surface of V13D NTD upon binding to D70K NTD using NMR-based titration. In this experiment, ^{15}N-labeled V13D NTD was titrated with unlabeled D70K NTD. Panels *A*-*D* show the HSQC spectra of V13D NTD with increasing molar ratio of D70K NTD. A selected set of peaks from V13D NTD (highlighted with red ovals) became weak upon addition of D70K NTD and eventually completely disappeared during titration. The chemical shift assignment of V13D NTD is labeled in panel *A*.

Figure 6. Mapping of the V13D NTD binding surface on D70K NTD by NMR spectroscopy. In this experiment, ^{15}N-labeled D70K NTD was titrated with unlabeled V13D NTD, and the HSQC spectra of D70K NTD in the presence of different molar ratios of V13D NTD are superimposed on to each other. A selected set of peaks from D70K NTD (peaks highlighted by arrows) underwent dose-dependent chemical shift changes upon binding to V13D NTD. The shift assignment of D70K NTD is also

labeled.

Figure 7. Mapping the interaction interface between two NTD monomers. (A) Overlay plot of the spectra of ^{15}N-labeled V13D NTD in the presence equal molar amount of unlabeled, Cys6 EDTA-tagged D70K saturated with diamagnetic Y^{3+} or paramagnetic Dy^{3+}. Addition of paramagnetic Dy^{3+} induces line broadening and chemical shift changes to a subset of peaks in the ^{15}N-labeled V13D NTD. To tag EDTA onto D70K NTD, purified D70K NTD with single Cys6 (in 50 mM Tris buffer, pH 7.4, containing 100mM NaCl) was incubated with 10 fold excessive of S-(2-pyridylthione)-cysteaminyl-EDTA at 4℃ overnight. The labeled protein was separated with the excess EDTA derivatives with a PD-10 desalting column. Ellman's assay was used to monitor the completeness of the labeling. (B) The surface charge representation of B1 and B2 sites of NTD. The position of Cys6 used for paramagnetic tagging is labeled with a star. (C) Mapping Dy^{3+}-induced chemical shift changes on to the acidic surface of neighboring NTD unit. It is clear that the paramagnetic shifts induced by Dy^{3+} tagged in the B1 site in the neighboring NTD are limited to the residues within or surrounding the A1 site, indicating that the residues in B1 region of D70K NTD is in contact with the residues in the A1 region of V13D NTD. (D) Mapping Dy^{3+}-induced chemical shift changes on to the NTD dimer model. Cys6 in D70K NTD used for paramagnetic tagging is shown in explicit atomic representation. Dy^{3+}-induced chemical shift changes observed in ^{15}N-labeled V13D NTD is colored. (E) Gel filtration profiles of the wild type NTD and R33Q/K36Q

NTD at a protein concentration of 15mg/ml. The majority of the wild type NTD was eluted at the void volume of the column. The R33Q/K36Q NTD was eluted as a single population of monomer, indicating the mutations disrupted NTD multimerization. The data support the NTD dimer model shown in panel D. In contrast, if two neighboring NTD interacts via B1-A2 and B2-A1 pairwise interactions (i.e., one of the NTD unit in the dimer model in panel *D* needs to rotate ~180°), the surface complementation between B1 and A2 is reasonably good, but the complementation between B2 and A1 is compromised leaving Arg33 and Lys36 solvent exposed. Mutation of these two residues to Gln is not expected to have significant impact on the multimerization of NTD in the second hypothetical model.

Figure 8. Modeling of Par-3 NTD onto a the Par-6/aPKC PB1 heterodimer. (A) Par-3 NTD (purple) was superimposed on to the Par-6 PB1 domain (orange) with their respective secondary structures. In this Par-3 NTD/aPKC PB1 heterodimer model, the elongated α1 of Par-3 NTD crashes with the β4/α2-loop and β3 of aPKC PB1 domain. (B) Par-3 NTD (purple) was superimposed on to the aPKC PB1 domain (green) with their respective secondary structures. In this heterodimer model, the Par-3 NTD and the Par-6 PB1 lacks surface as well as charge complementation due to the short α2 helix and the short β3/β4-loop of Par-3 NTD.

Figure 9. Electron microscopic studies of Par-3 (1-704). (A) The wild type Par-3(1-704) forms fiber structure under EM. In contrast, V13D Par-3(1-704) and

V13D/D70K Par-3(1-704) do not form fiber structure under EM. (B) SDS-PAGE showing the purification of the wild type, V13D, and V13D/D70K Par-3(1-704) proteins. The purity of the proteins used for EM studies is about ~90%.

Supplementary Table 1. Summary of characterization of NTD mutants

Mutation site	Screened NTD Mutants	Protein behavior category
Mutation on positive pocket (blue)	V13D	★
	R33Q/K36Q	★
Mutation on hydrophobic residues or Cys (magenta)	F24S	▽
	C6/16S	▽
	C66S	▽
	V38S	▽
	V68S	▽
	V68K	▽
	A69K	▽
	V78S	▽
Mutation on negative pocket (red)	I58K	■
	I58S	■
	D67A	◇
	D67K	◇
	D73K	▽
	D60K	■
	I58S/D67A	■
	I58S/D70K	★
	I58K/D70K	★
	I58K/D60S	■
	I58S/D69K	■
	D70A	★
	D70K	★
	D62/62A	■
	D60/62K	■
	D62/63K	◇
	D62/63/70K	◇
	D62/63/80K	▽
	D62/63/70/80K	▽
	D60/62/70K	■
	D60/70K	★
Mutation on both positive and negative pocket (blue&red)	V13D/D70K	★

★ Monomeric mutants/highly soluble/stable/well folded
■ Oligomeric mutants/highly soluble/stable
◇ Oligomeric mutants/highly soluble/unstable/precipitation
▽ Highly insoluble/low yield/unstable/precipitation

Supplementary Figure 1

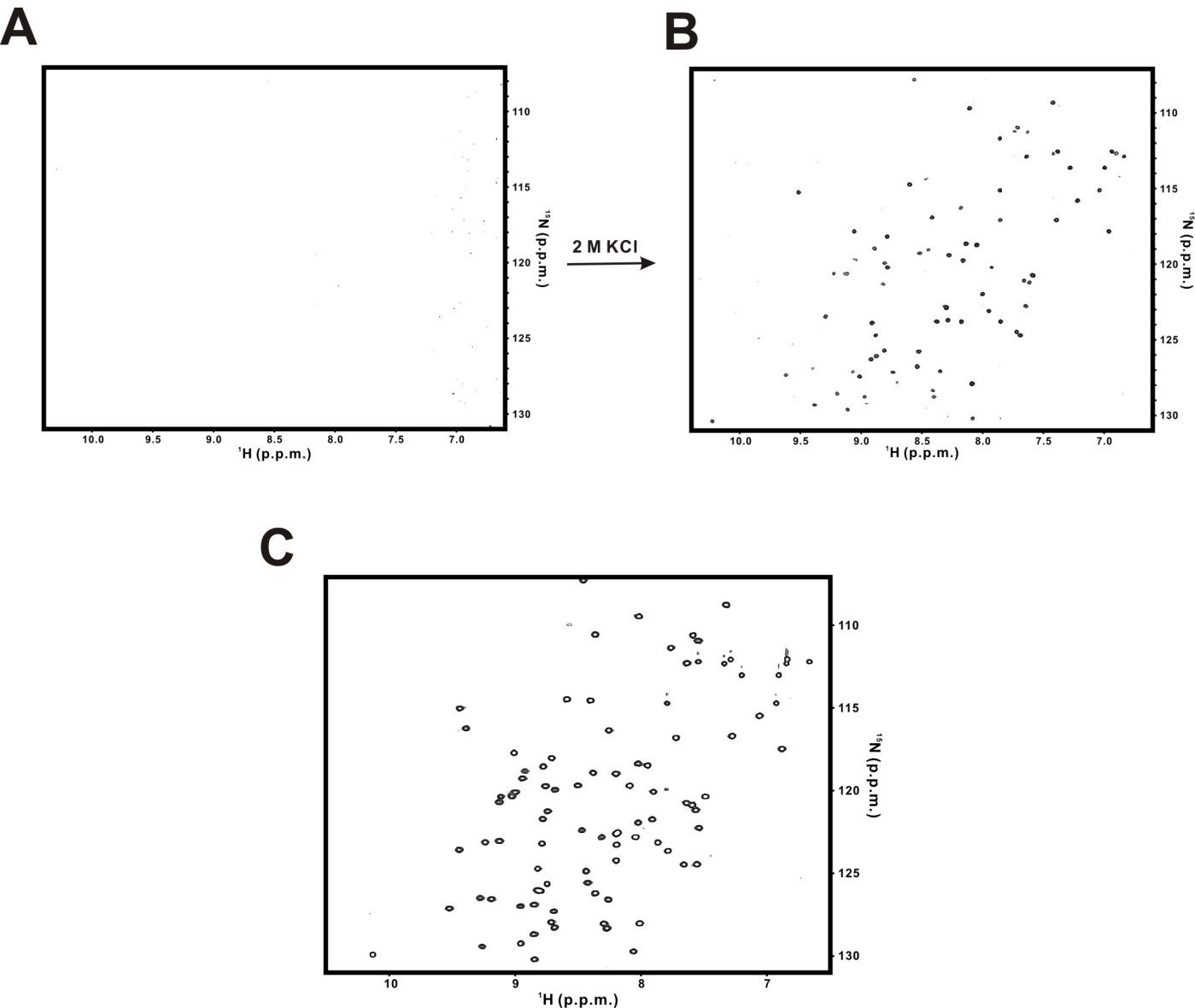

Supplementary Figure 2

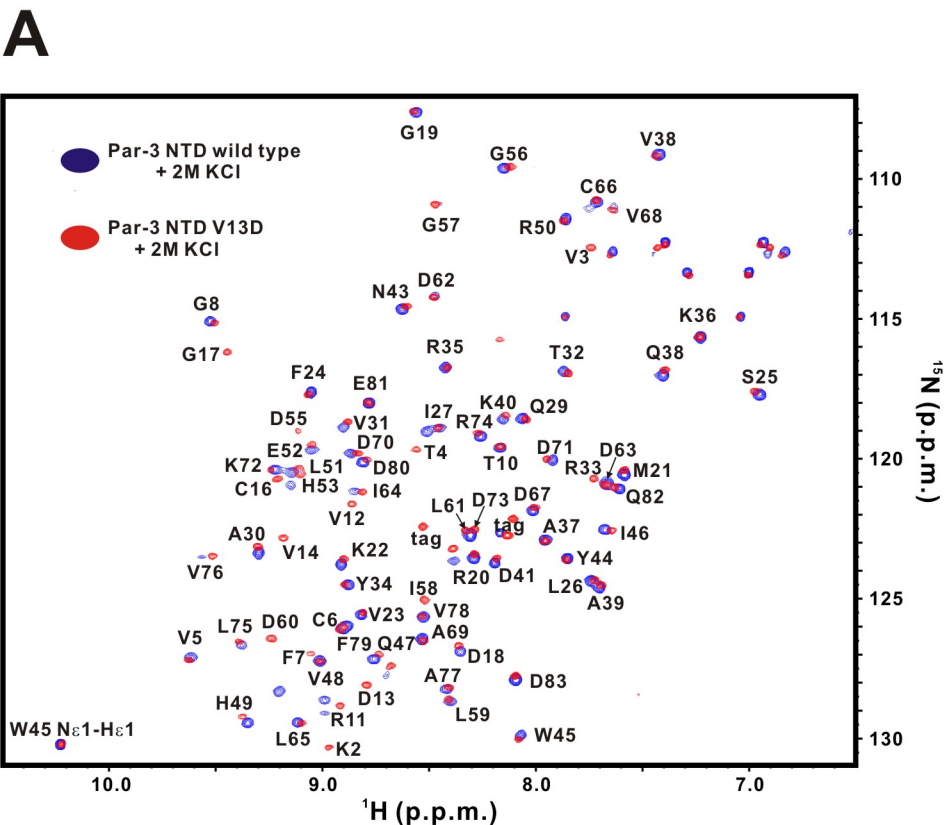

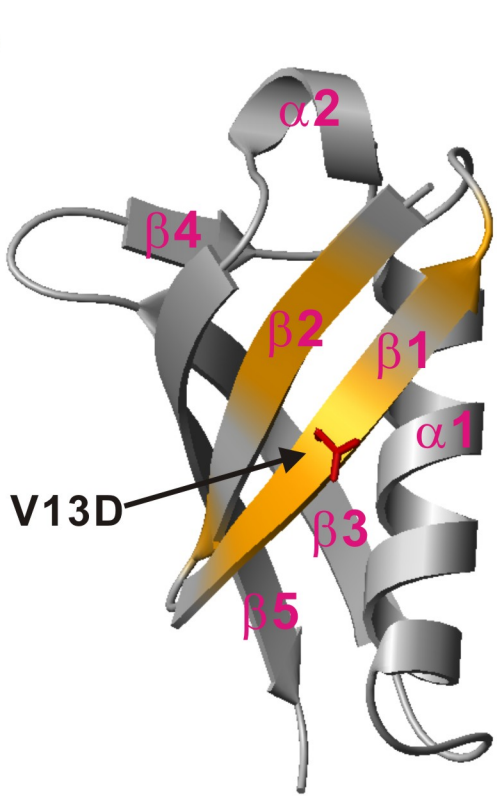

Supplementary Figure 3

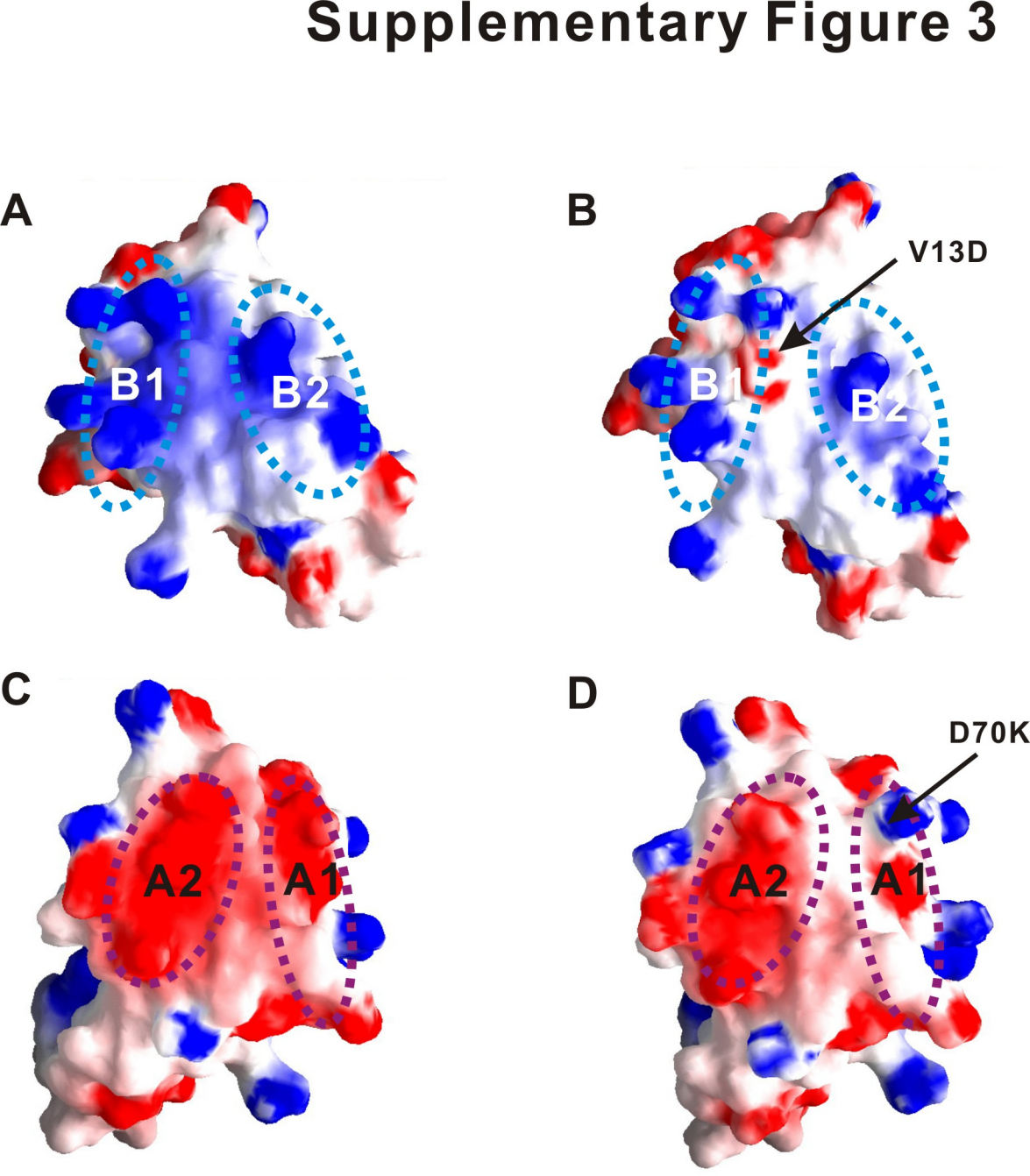

Supplementary Figure 4

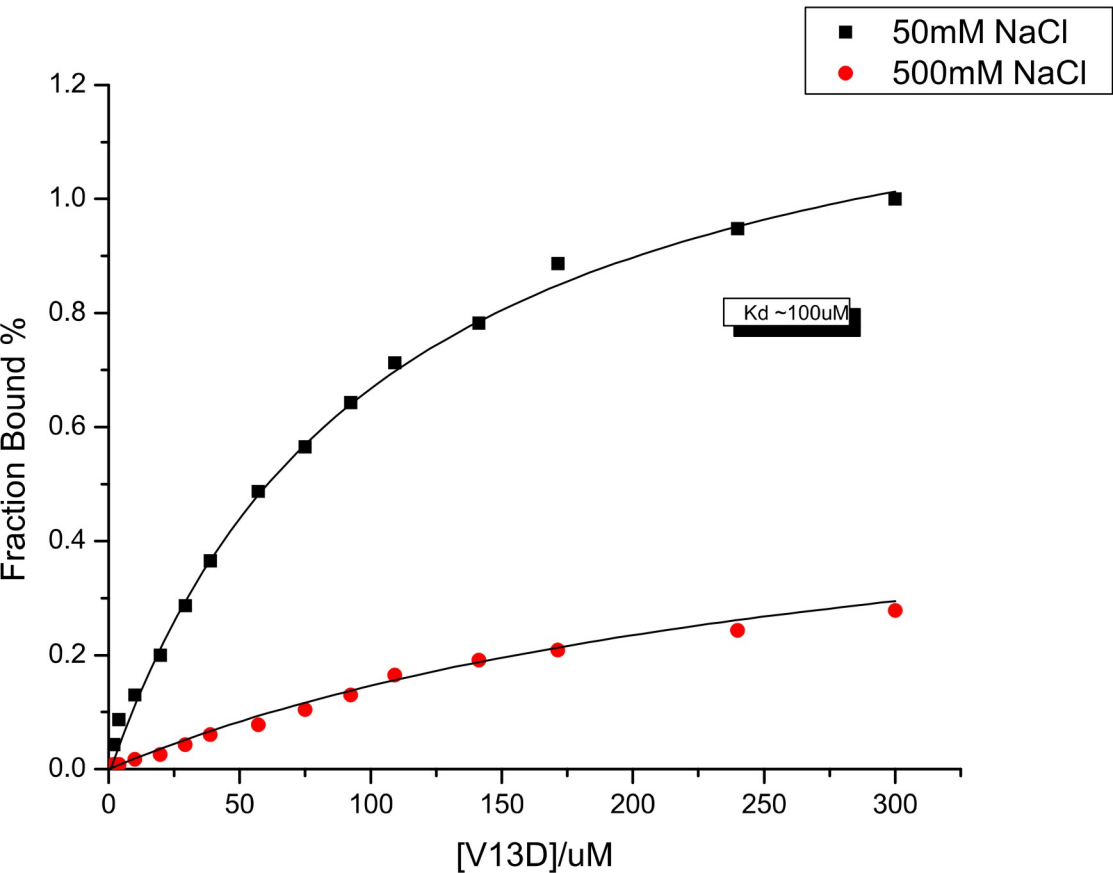

Supplementary Figure 5

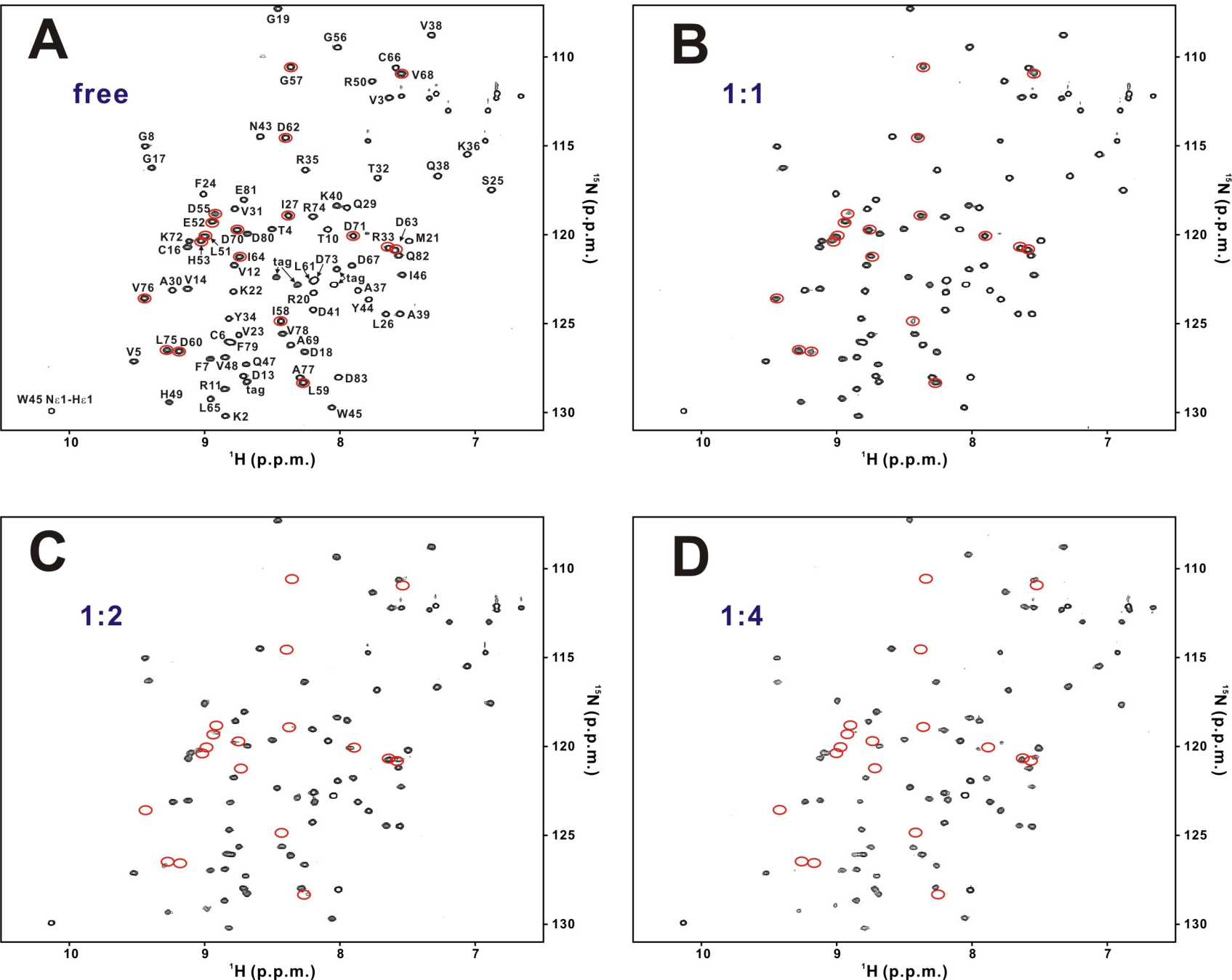

Supplementary Figure 6

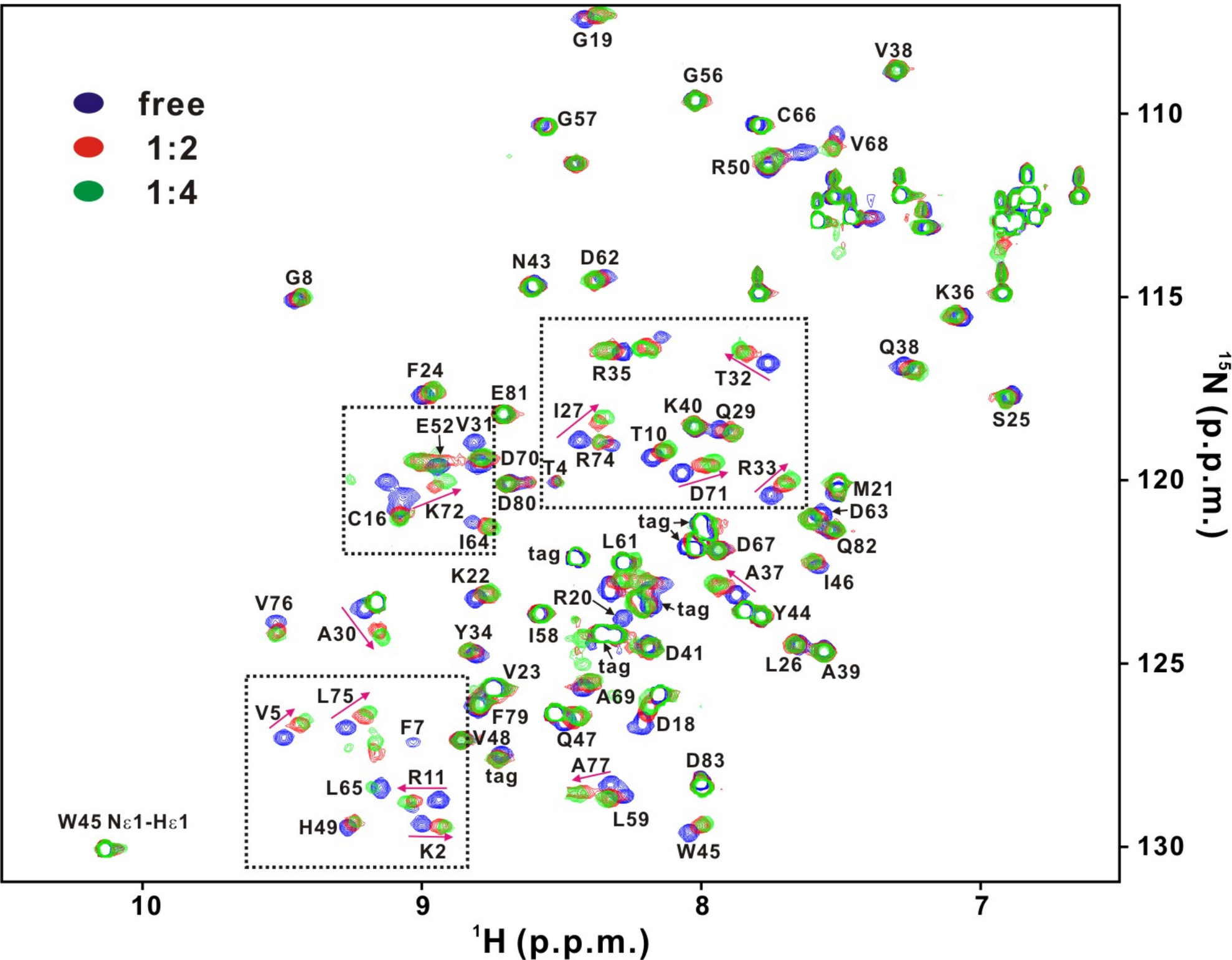

Supplementary Figure 7

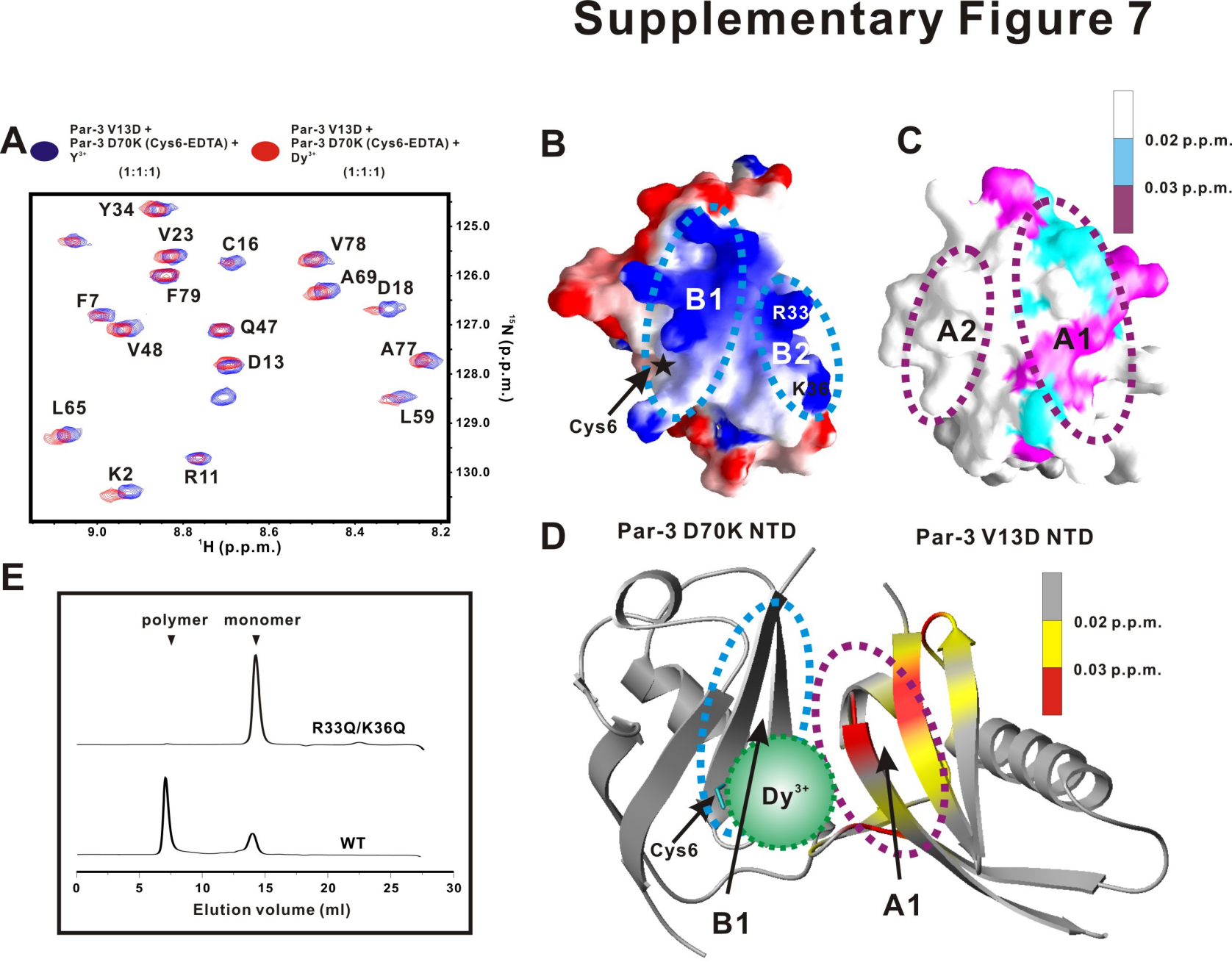

Supplementary Figure 8

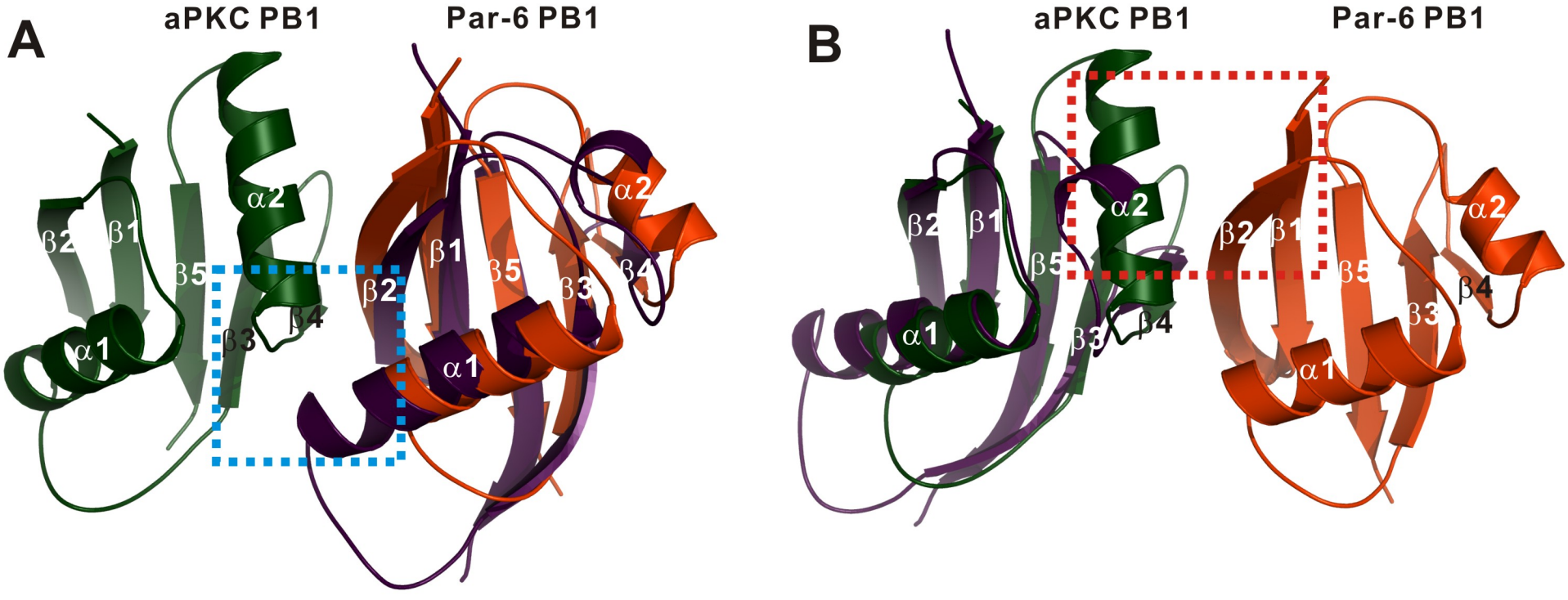

Supplementary Figure 9